Active Flutter Suppression Using Eigenspace and Linear Quadratic Design Techniques

William L. Garrard* and Bradley S. Liebst†
University of Minnesota, Minneapolis, Minnesota

Eigenspace and linear quadratic techniques are used to design an active flutter suppression system for the DAST ARW-2 flight test vehicle. Outboard and inboard control surfaces are included in the design. Flutter controllers that meet control surface activity specifications and provide some gust load alleviation are developed using both eigenspace and linear quadratic techniques. However, inclusion of the inboard control surface is shown to yield substantial design compromises in terms of closed-loop actuator response in the case of linear quadratic design and stability margins in the case of eigenspace design.

Nomenclature

Vectors

u	= control input
v_i	= attainable closed-loop eigenvector associated with λ_i eigenvalue
v_{d_i}	= desired closed-loop eigenvector associated with λ_i eigenvalue
w_i	= vector used in calculation of eigenspace gain matrix, see Eq. (17)
x	= system state
ξ_F	= flexure modal displacement
ξ_c	= control surface displacements
Γ	= disturbance input vector

Matrices

$[A_m]$	= aerodynamic coefficient matrix
A	= dynamics matrix
B	= control distribution matrix
$[C_s]$	= structural damping matrix
E	= aerodynamic coefficient error matrix
K	= control gain matrix
L_i	= matrix relating v_i and w_i, see Eq. (15)
$[K_s]$	= structural stiffness matrix
$[M_s]$	= structural mass matrix
P_i	= eigenvector weighting matrix
Q	= state weighting matrix
$[Q_c]$	= calculated unsteady aerodynamic influence coefficient matrix
$[Q_A]$	= s-plane representation of unsteady aerodynamic influence coefficient matrix
R	= control weighting matrix
V	= matrix whose columns are v_i
W	= matrix whose columns are w_i

Scalars

c	= reference chord, 0.6 m
$H(s)G(s)$	= loop transfer function
j	= $\sqrt{-1}$
J	= linear quadratic performance index
k	= reduced frequency
L	= reference length in gust model, 762 m
M	= Mach number
q	= dynamic pressure
s	= Laplace operator
V	= forward velocity
β_m	= aerodynamic lag frequencies
η	= zero mean white noise input to gust model with intensity, $(L/V)\bar{\xi}_G^2$
λ_i	= ith eigenvalue
$\bar{\sigma}(E)$	= maximum singular value of E
$\underline{\sigma}(E)$	= minimum singular value of E
ω	= circular frequency
ξ_G	= normal wind gust velocity
$\bar{\xi}_G$	= rms normal wind gust velocity

Subscripts

i	= inboard aileron
o	= outboard aileron
ES	= eigenspace
LQ	= linear quadratic
s	= structural

Superscripts

$(\ )^*$	= complex conjugate transpose
T	= transpose

Introduction

THE objective of this paper is to examine the application of eigenspace (ES) and linear quadratic (LQ) techniques to the preliminary design of an active flutter suppression system for a flight test vehicle. There has been considerable interest in the application of LQ techniques to the design of active flutter suppression systems. Much of this work has focused on the DAST flight test vehicles,[1-5] although future transport-type aircraft have also been considered.[6,7] ES techniques, which use feedback control to directly place closed-loop eigenvalues and shape closed-loop eigenvectors,[8] have not been extensively applied to the design of active flutter control systems. Ostroff and Pines[9] used eigenvalue placement to design a flutter controller, but did not attempt to shape the closed-loop eigenvectors. In this paper, an ES design procedure is developed for active flutter suppression. This technique and standard LQ synthesis procedures are applied to the design of a flutter suppression system for the DAST ARW-2 flight test vehicle and the results are compared.

Both LQ and ES techniques result in full-state feedback control laws. Since accelerometers are used to determine the motion of the wing, the system states are not measured

---

Received Feb. 3, 1983; revision received Nov. 9, 1983.

*Associate Professor, Department of Aerospace Engineering and Mechanics. Associate Fellow AIAA.

†Assistant Professor, Department of Aerospace Engineering and Mechanics. Member AIAA.

directly and a dynamic compensator must be used to convert the accelerometer outputs to control inputs. Compensator design may be accomplished by the use of state observors (including Kalman filters)[4-7,10] or frequency response matching techniques.[2] In either case, it is necessary to have full-state control laws that yield acceptable performance. In the preliminary design stage, it is useful to compare the performance of full-state controllers in order to identify those designs that warrant further development. Since this paper is concerned with preliminary design configurations and comparisons of controllers resulting from two design methodologies, only full-state feedback is considered. The author's current research efforts are focused on the development of suitable compensator designs.

Performance Requirements and System Model

The DAST ARW-2 flight test vehicle is a Firebee II drone that has been modified by replacing the conventional wing with a high-aspect-ratio supercritical wing designed to flutter within the flight envelope. Two control surfaces, inboard and outboard ailerons, are available on the wing. Although current plans are to use the outboard aileron for flutter control and the inboard aileron for maneuver load alleviation, the inboard aileron was included in the flutter control system developed in this paper. It was felt that a system using both control surfaces might exhibit improved performance compared with a system using only the outboard aileron; the inboard aileron might also provide a redundant control surface in case of failure of the outboard aileron. In addition, inclusion of the inboard aileron results in a system with multiple (two) control inputs. This allows an additional flexibility in the controller design not available in single-input systems.

The design flight condition for the flutter control system is a velocity of 275 m/s (Mach 0.86) and an altitude of 4572 m (15,000 ft). At this flight condition, the uncontrolled wing flutters, and the flutter control system is required to stabilize the wing without exceeding specified limits on rms control surface activity. The rms deflection of the inboard aileron is limited to 10 deg and the deflection rate to 130 deg/s. The rms deflection of the outboard aileron is limited to 15 deg and the deflection rate to 740 deg/s. The control surfaces saturate if these limits are exceeded. In addition, gain margins of at least 6 dB and phase margins of at least 45 deg are desirable.

The wing flutters at a velocity of 240 m/s (Mach 0.75) at an altitude of 4572 m and the flutter controller is activated at a velocity of about 226 m/s (Mach 0.7). Thus, the performance

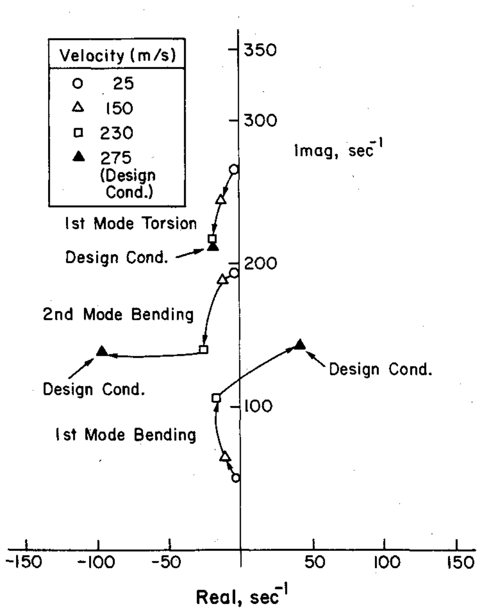

Fig. 1 Root loci of uncontrolled wing as velocity is varied.

of the flutter control system is evaluated at this flight condition as well as the design condition of Mach 0.86. Since the uncontrolled wing is stable at Mach 0.7 and 4572 m, it must be verified that activation of the control system does not destabilize the wing. Furthermore, the flutter controller should not result in excessive increases in the bending, torsional, or shear loads compared with the uncontrolled wing. In the actual DAST vehicle, an independent gust load alleviation system is also to be evaluated at the Mach 0.7, 4572 m flight condition; therefore, this condition will be referred to as the gust test condition in the sequel, even though the gust load alleviation system is not discussed in this paper.

The aeroelastic model of the wing is given as

$$([M_s]s^2+[C_s]s+[K_s])[\xi_F]+q[Q_c(s)]\left|\begin{matrix}\xi_F\\ \xi_c\\ \dfrac{\xi_G}{V}\end{matrix}\right| = 0 \tag{1}$$

where $[Q_c(s)]$ is approximated by

$$[Q_A(s)] = [A_0]+[A_1]\frac{cs}{2V}+[A_2]\left[\frac{cs^2}{2V}\right] + \sum_{m=1}^{L}\frac{[A_{m+2}]s}{s+(2V/c)\beta_m} \tag{2}$$

This approximation has been widely used in the design of active flutter suppression systems.[2-7,11] The usual procedure[4] is to select the β_m in such a way as to bracket the reduced flutter frequency and then choose the $[A_m]$ matrices so as to give the best least squares fit to $[Q_c]$ over a range of reduced frequencies. The aerodynamic influence matrix $[Q_c]$ is calculated as a function of reduced frequency by a doublet-lattice procedure.

In this study, a new method was used to select the β_m.[12] An error matrix was defined as

$$E(j\omega)=[Q_c(j\omega)]-[Q_A(j\omega)] \tag{3}$$

The norm of this matrix is bounded above and below by its maximum and minimum singular values,[13] i.e.,

$$\underline{\sigma}(E)\le\frac{\|Ex\|}{\|x\|}\le\bar{\sigma}(E)$$

The singular values of E are defined as the positive square roots of the eigenvalues of E^*E. If the β_m are chosen to minimize $\bar{\sigma}(E)$, the norm of the error matrix will be small.

In this study, a single β was used in $[Q_A]$. Since the reduced flutter frequency was known to be small, β was selected to minimize $\bar{\sigma}(E)$ at zero frequency. The resulting value of β was 0.13, which is very close to the reduced flutter frequency of 0.15. The eigenvalues obtained from this model were almost identical to those calculated from a higher-order model that included several lag frequencies.[12] Also, the elements of the $[Q_A]$ matrix were very close to those of the $[Q_c]$ matrix when compared over reduced frequencies of 0.0-1.2. The poorest correlation between elements of the $[Q_c]$ and $[Q_A]$ matrices occurred for the coefficients associated with the gust velocity. Even then, the rms control surface gust responses calculated using the model with a single β were close to those calculated from higher-order models using several values of β_m.

It is felt that selection of the numerical values of the β_m based on the maximum and minimum singular values of an error matrix such as given by Eq. (3) has considerable potential in generating low-order approximate models of unsteady aerodynamics. Even the simple approach of minimizing the maximum singular value of the error matrix at a fixed frequency yielded acceptable results. Other approaches, such as choosing the β_m to minimize both the maximum and minimum singular values over a range of frequencies, are currently being investigated.

Initially, seven structural modes were used in the mathematical model of the wing; however, by comparing the eigenvalues calculated using lower-order models with those resulting from a model that included seven structural modes, it was found that flutter could accurately be modeled by including only three modes. These modes corresponded to first and second bending and first torsion.[12] Since computational expense could be reduced significantly by reducing the order of the system model, subsequent design studies and system performance evaluations were based on a structural model containing only these three modes. The loci of the roots associated with these flexure modes are given as functions of velocity in Fig. 1. The lowest frequency mode is associated with first-mode bending, the next highest with second-mode bending, and the highest is first-mode torsion. It can be seen that first-mode bending is the unstable mode, whereas second-mode damping increases with velocity. The frequencies of these two modes approach one another with increasing velocity. The first torsion mode is not affected by velocity as much as the two bending modes, but it is necessary to include this mode in order for the system to flutter.

The wind gust model is taken from Houbolt et al.[15] The transfer function for this model is

$$\xi_G(s)/\eta(s) = [1+(\sqrt{3}L/V)s]/[1+(L/V)s]^2 \tag{4}$$

The rms gust velocity is 3.6 m/s (12 ft/s).

Both inboard and outboard ailerons are driven by high-band width hydraulic actuators. In the range of frequencies covered by the three-mode structural model, a fourth-order transfer function gives a very close approximation of the actual inboard aileron/actuator transfer function.[14] This transfer function is

$$\xi_{c_i}(s)/u_i(s) = 1.7576637\times 10^{11}/[s^2+671s + (477.5)^2][s^2+322s+(878)^2] \tag{5}$$

A third-order transfer function is used for the outboard actuator. This transfer function is

$$\xi_{c_0}(s)/u_0(s) = 1.7747280\times 10^{7}/(s + 180)[s^2+251s+(314)^2] \tag{6}$$

Both transfer functions have unity gain at zero frequency.

Equations (1), (2), and (4-6) can be combined to give the equations describing the wing, control surfaces and actuators, and wind gust in vector-matrix form as

$$\dot{x} = Ax + Bu + \Gamma\eta \tag{7}$$

The 18th-order state vector x consists of the displacements and velocities associated with the three flexure modes, the unsteady aerodynamic lag states, the states associated with the inboard and outboard control surfaces, and the states associated with the wind gust model. The second-order control vector u consists of the commanded inputs to the inboard and outboard aileron/actuators and the scalar white noise input η drives the wind gust model. Numerical values for the elements of the A, B, and Γ matrices are given in Ref. 16.

Controller Design Methodology

Linear quadratic control theory has been discussed in numerous texts, e.g., Ref. 17. The basic LQ design procedure consists of selecting quadratic weighting matrices Q and R in a scalar performance index

$$J = \frac{1}{2}\int_0^\infty [x^TQx + u^TRu]\,\mathrm{d}t \tag{8}$$

The control minimizing this performance index is given as

$$u = Kx \tag{9}$$

where the gain matrix K is obtained from the solution of a matrix Ricatti equation. The usual procedure is to iteratively vary Q and R until performance specifications on rms values of the state and control are met.

Eigenspace design methodology has received less attention than LQ techniques, but is still well known. Moore[8] and others have shown how feedback can be used to directly place eigenvalues and also shape eigenvectors. If performance specifications are given or can be interpreted in terms of desired closed-loop eigenvalues and eigenvectors, then ES techniques can provide a natural design procedure where the desired eigenstructure (if obtainable) can be calculated without iteration. If performance specifications cannot be clearly stated in terms of closed-loop eigenvalues and eigenvectors (for example, specifications on rms responses), it may be necessary to iterate eigenvalues and eigenvectors until the performance specifications are met. In the discussion below, full-state feedback is assumed.

If there is one independent control for each state, then all of the controllable eigenvalues and eigenvectors can be placed arbitrarily.[8] Since there are almost always fewer controls than states, not all of the eigenvalues and eigenvectors can be placed. The design procedure then becomes one of placing eigenvalues and shaping eigenvectors to eliminate certain state responses from a mode while emphasizing others. This procedure has been successfully demonstrated by Cunningham[18] in decoupling aircraft rigid-body modes.

The ES design procedure consists of determining a gain matrix K such that for all desired closed-loop eigenvalue λ_i and eigenvector v_i pairs

$$(A+BK)v_i = \lambda_i v_i \tag{10}$$

This is equivalent to finding w_i, such that

$$(\lambda_i I - A)v_i = Bw_i \tag{11}$$

Once the w_i have been found, the gain matrix is calculated as

$$K = WV^{-1} \tag{12}$$

If it is desired to change an eigenvalue associated with a controllable mode, then for the new eigenvalue λ_i the matrix $(\lambda_i I - A)$ is nonsingular. Thus,

$$v_i = (\lambda_i I - A)^{-1}Bw_i \tag{13}$$

or

$$v_i = L_i w_i \tag{14}$$

where

$$L_i = (\lambda_i I - A)^{-1}B \tag{15}$$

Since in general there are not enough independent controls available to arbitrarily place all λ_i and v_i, the w_i are selected to minimize the following least square performance index:

$$J_i = (v_{d_i} - v_i)^* P_i (v_{d_i} - v_i) \tag{16}$$

where P_i is used to emphasize certain components of v_{d_i}. Solving for w_i which minimizes J_i produces an optimal pseudoinverse

$$w_i = (L_i^* P_i L_i)^{-1} L_i^* P_i v_{d_i} \tag{17}$$

and v_i is given by Eq. (13).

If certain eigensolutions are not to be altered or if λ_i is uncontrollable, then

$$w_i = 0$$

and Eq. (11) is satisfied. The general design procedure used is to vary P_i, λ_i, and v_{d_i} until the performance specifications on the rms values of the state and control are met.

There is obviously a relationship between the LQ and ES design techniques. Harvey and Stein[19,20] have shown how quadratic weights in the performance index given by Eq. (8) can be selected so that the closed-loop eigenstructure resulting from use of LQ design methodology asymptotically approaches some desired eigenstructure. However, this procedure drives those eigenvalues not specified asymptotically to infinity. This may not be desirable in terms of practical control system realization. Also, if a given eigenstructure is desired, it seems simplest to calculate directly the required feedback gains rather than to approach them iteratively via asymptotic LQ theory. If the closed-loop LQ eigenstructure is specified, ES design techniques can be used to determine a gain matrix that yields this eigenstructure, although this gain matrix is not necessarily unique except in the single-input/single-output case.

In the remainder of this paper, both the LQ and ES design techniques will be applied to the design of a flutter controller for the system modeled in the previous section. It would be impossible to conclude that one method is better than the other, since the ES controller would result if proper Q and R matrices were selected in the LQ design procedure and the LQ eigenstructure can be obtained by ES design techniques. In fact, both controllers are similar and it is felt that a study of the results in this paper gives considerable insight into the design of flutter controllers. Also, since the design methodology for ES controllers of flutter suppression and other aeroelastic control problems is not yet well defined, it is thought that the ES design procedure described below should be of interest.

Linear Quadratic Controller Design

It is well known that if Q is set equal to zero and R equal to the identity matrix in the performance index given by Eq. (8), all stable eigenvalues will remain unchanged and all unstable eigenvalues will be rotated about the imaginary axis.[17] Initial LQ design was performed using this approach; however, as shown in Tables 1 and 2, the rms deflection rate for the inboard actuator was approximately double its allowed maximum at the flutter test condition and, at the Mach 0.7 condition, two of the closed-loop eigenvalues associated with the inboard actuator were unstable. Over 25 combinations of Q and R matrices were evaluated in an attempt to improve the design.[16]

The best results were obtained by maintaining R as the identity matrix and weighting only the inboard actuator deflection rate in the Q matrix. The results of varying this weight are shown in Table 1. The rms value of the inboard actuator deflection rate decreases fairly rapidly as its weight is increased and the rms activity level of the outboard aileron does not change greatly as the weight on the inboard actuator rate is changed. The feedback gains associated with the inboard actuator states increase rapidly with the weight on the inboard actuator rate. As shown in Fig. 2, the eigenvalues associated with the inboard actuator change radically. The moduli of three of the roots become very large, while the fourth root approaches zero. Since any large change in actuator frequency response characteristics would be difficult to obtain without substantially redesigning the actuator, a value for the weight on inboard actuator deflection rate of 1×10^{-4} was selected. Since the magnitude of the inboard deflection rate is of order 100 times the inboard deflection, this results in x^TQx of the same order of magnitude as u^TRu in Eq. (8).

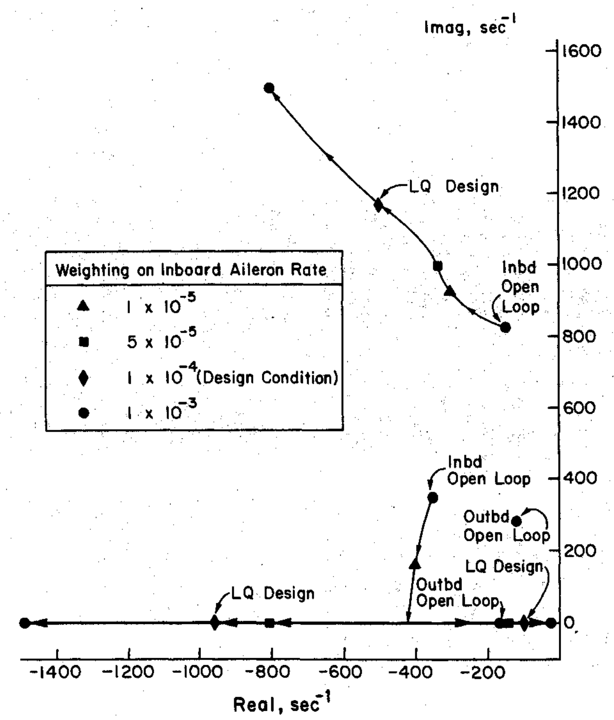

Fig. 2 Variation in actuator roots with weighting on inboard aileron deflection.

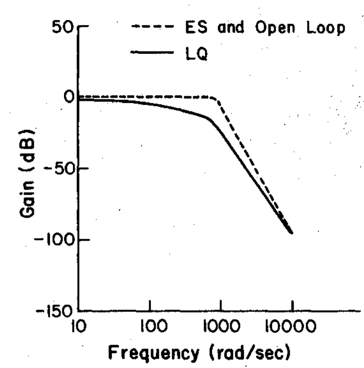

Fig. 3 Inboard actuator transfer function frequency response with and without external actuator feedback.

The resulting design gave acceptable rms responses at the design condition and a stable system at the gust test condition. Inboard actuator open- and closed-loop frequency responses for the final LQ design are shown in Fig. 3. It can be seen that the overall gain for the closed-loop system is reduced compared with the open-loop response. At zero frequency, the open-loop gain is unity and the closed-loop gain is 0.79. Thus, the forward-loop gain would have to be increased by 21% in order to restore the steady-state gain to its open-loop value. This might be difficult without modifying existing actuator hardware.

Eigenspace Controller Design

As for the initial LQ design, the initial ES controller was designed by rotating the unstable eigenvalues around the imaginary axis and leaving all other eigensolutions in their open-loop configuration. This resulted in acceptable rms control surface activity at the flutter condition and a stable response at the gust test condition. It is interesting to note that, although the eigenvalues of both the initial LQ and ES designs were the same, the feedback gain matrices were different, resulting in different dynamic response characteristics. Although the initial ES design stabilized the wing at both the flutter and the gust test conditions, the rms inboard deflection rate is near its maximum value at the flutter condition. It was felt that the performance might be enhanced by redesign of the control system so as to reduce the inboard deflection rate. Since the aircraft exhibits satisfactory response at velocities somewhat less than the flutter speed, it was decided to use ES design techniques to force the closed-loop response of the wing at the design velocity to approach the open-loop response of the wing at a velocity of 200 m/s (20% less than the flutter speed).

The ES design procedure described previously was used to synthesize a gain matrix that forced the closed-loop eigenvalues associated with the controllable states of the wing at the design velocity (275 m/s) to be the same as the open-loop eigenvalues of the wing at 200 m/s. The open-loop actuator eigenvalues are the same for both flight conditions and were not moved. The ability to maintain actuator eigenvalues in their open-loop positions is one of the major advantages of the eigenspace design. The closed-loop frequency response of the actuator with the ES controller is shown in Fig. 3 and is identical to the open-loop response. The gust states are not controllable and their eigenvalues cannot be moved. The desired eigenvectors associated with the shifted eigenvalues were selected to be the same as the corresponding eigenvectors of the uncontrolled wing at 200 m/s. Initially, the weighting matrices P_i in the performance index given by Eq. (16) were chosen to be identity matrices. That is, the control acted to minimize the scalar product of the difference between the desired and attainable closed-loop eigenvectors associated with each eigenvalue moved.

Table 1 RMS responses at flutter condition for various weights on inboard actuator rate

Weight on inbd deflection rate	RMS response, deg and deg/s			
	Inbd def.	Inbd rate	Outbd def.	Outbd rate
0	1.60	271.6	2.73	427
1×10^{-5}	1.58	256.0	2.74	428
5×10^{-5}	0.92	122.0	3.02	470
1×10^{-4}	0.66	84.8	3.14	486
5×10^{-4}	0.22	26.0	3.32	514
1×10^{-3}	0.12	14.0	3.36	518
Max allowable	10.0	130.0	15.0	740

It was found that this procedure reduced all control surface activity by about 7%. Since the inboard rate was still close to its maximum allowable value, it was decided to shift some control surface activity from the inboard to the outboard actuator. This was accomplished as follows. The components of the open-loop aeroelastic eigenvectors in the actuator directions are zero for all flight conditions. The desired eigenvectors were chosen to be the open-loop eigenvectors at a velocity of 200 m/s; thus, by penalizing the components of the difference between the actual and desired aeroelastic eigenvectors in the direction of the inboard actuator, inboard control activity should be reduced. This was accomplished by increasing the weights placed on the difference between the actual and desired components of each aeroelastic eigenvector in the direction of the inboard rate. Values of the weights on these components were iteratively increased from 1 to 2.5×10^3, while all of the other weights were maintained at 1. The final result is shown in Table 2.

The inboard rate was reduced substantially and the inboard deflection and outboard deflection and rate were increased, indicating that the eigenspace design procedure given here does shape the response as desired. It proved possible to reduce the inboard rate still further by increasing the elements of the P_i matrix that weight the difference between the components in the inboard rate direction of the actual and desired closed-loop aeroelastic eigenvectors. However, the outboard rate then begins to approach its maximum value.

Results

The closed-loop flutter characteristics for the LQ and ES designs are similar. The root locus of the eigenvalues of the wing with the LQ controller is shown in Fig. 4 as velocity is varied. The wing becomes unstable at a velocity of about 295 m/s (the design condition was 275 m/s and the uncontrolled flutter speed was 240 m/s). It is interesting to note that one of the roots associated with the unsteady aerodynamic lag states also becomes unstable, resulting in divergence; whereas in the uncontrolled case, the first bending mode becomes unstable in classical coupled mode flutter (Fig. 1). The root locus for the ES design is shown in Fig. 5. For the ES controller, the wing becomes unstable at a velocity of about 310 m/s. As in the uncontrolled case, the first bending mode becomes unstable; but in the controlled case, the eigenvalues associated with this

Table 2 Comparison of rms control surface activity for various controller designs and flight conditions

Controller design	Inbd defl, deg		Inbd rate, deg/s		Outbd defl, deg		Outbd rate, deg/s	
	Flutter	Gust test	Flutter	Gust test	Flutter	Gust test	Flutter	Gust test
Unstable roots rotated about imag. axis								
ES	0.5	7.5	108.0	77.1	3.3	22.8	509.0	259.3
LQ	1.8	—[a]	271.0	—[a]	2.8	—[a]	407.0	—[a]
Eigenvector shaping to reduce inbd rate (final ES)	0.9	12.2	86.0	52.2	4.7	22.6	612.0	259.3
Weighting inbd rate in perf index (final LQ)	0.7	69	85.0	53.1	3.1	21.9	486.0	236.5
Final ES inbd failed	–	–	–	–	4.4	19.2	572.0	252.8
Final LQ inbd failed	–	–	–	–	3.5	21.8	519.0	249.8
Max allowable	10.0	10.0	130.0	130.0	15.0	15.0	740.0	740.0

[a]Unstable.

mode move to the real axis where one real root becomes unstable, resulting in divergence.

The results of varying altitude while maintaining Mach number constant are shown in Fig. 6. At $M=0.86$, the uncontrolled wing is unstable until an altitude of 6700 m is reached. At the same Mach number, the LQ controller results in a stable wing at all altitudes above 3200 m and the ES controller stabilizes the wing above altitudes of 2900 m. At $M=0.7$, the uncontrolled wing is stable for altitudes above 1800 m, whereas the ES controller stabilizes the wing for altitudes above 2100 m and the LQ controller stabilizes the wing for altitudes above 2400 m.

At the gust test condition, the outboard actuator deflection saturates at a gust of 3 m/s for all controller designs. However, if the rms gust velocity at the gust test condition is reduced to 2.5 m/s, both the ES and LQ controllers meet all specifications on rms surface activity. Table 3 shows that both controllers provide some torsional load alleviation at this flight condition. The bending and torsional moments and shear force were calculated at nine stations on the wing (station 1 is at the root and station 9 is near the tip). The LQ design results in the largest rms bending moments in the inboard region. The ES design results in bending moments that are lower than those resulting from the LQ design, but higher than the uncontrolled values. The differences in the bending moment in all three cases are not large. Both the LQ and ES designs result in substantial reductions (over 50%) in the torsional moments at all stations compared with the uncontrolled values. The LQ design reduces torsional moments slightly more than the ES design. The ES design results in the lowest value of shear near the wing root, but the uncontrolled values of shear are less near the tip. The differences in shear between the LQ, ES, and uncontrolled cases are not large at the gust test condition.

The ability of the ES and LQ systems to stabilize the wing in case of an actuator failure yielded little difference in the performance of the two systems. Actuator failure was simulated by assuming that the failed actuator control input was zero. When the outboard actuator failed, the inboard aileron was unable to stabilize the wing in both designs. When an inboard actuator failure was simulated, the outboard aileron was capable of stabilizing the wing with only small changes in the rms surface activity (see Table 2). In fact, with the ES controller, the rms responses improved slightly when the inboard actuator failed, indicating that the inboard control surface is not very useful for flutter suppression. The outboard aileron is critical in stabilizing the wing and it is important to examine the stability margins associated with the outboard control loop (the inboard actuator is assumed to be inoperative). This can be accomplished by examining the loop transfer function

$$H(s)G(s)=K[Is-A]^{-1}B$$

Note that, since $u=+Kx$, the characteristic equation is given by

$$1-H(s)G(s)=0$$

and the critical condition for stability occurs when the phase angle of $H(j\omega)G(j\omega)$ equals zero. For the LQ design,

$$H(s)G(s)_{\mathrm{LQ}}=\frac{-148.8(s-2.6)}{s^2-79.8s+(124.5)^2}$$

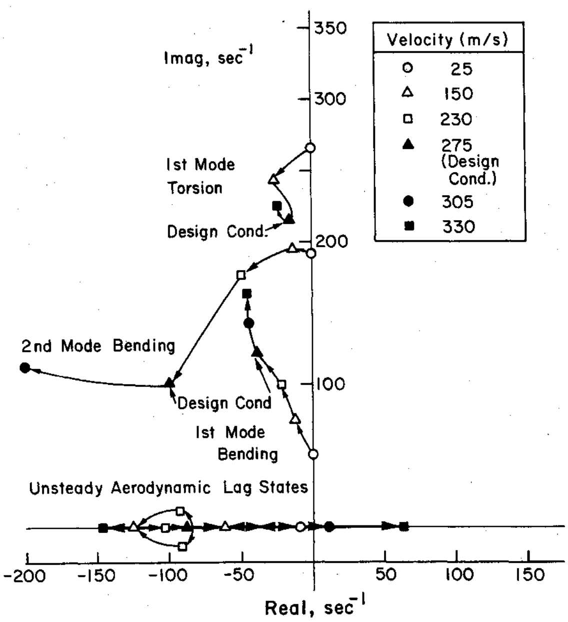

Fig. 4 Root locus of LQ controlled wing as velocity is varied.

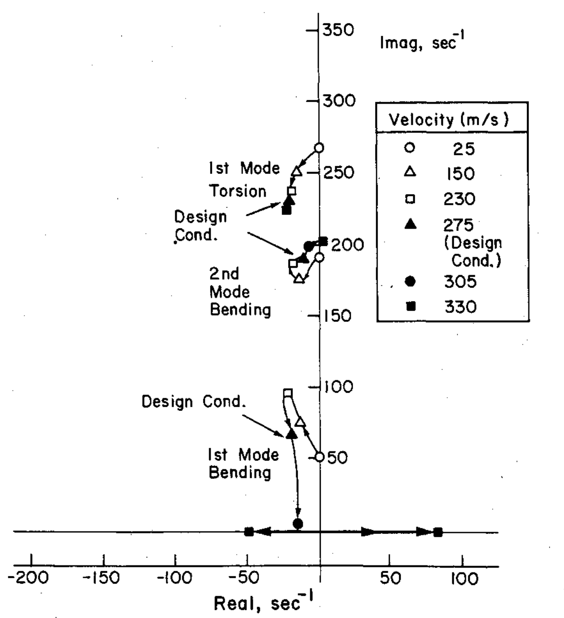

Fig. 5 Root locus of ES controlled wing as velocity is varied.

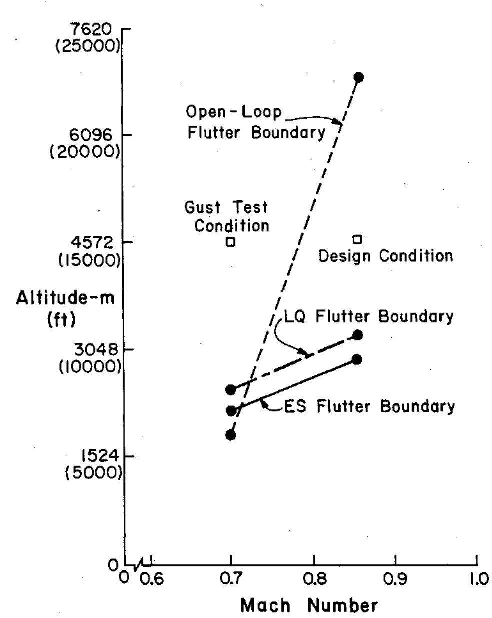

Fig. 6 Flutter boundaries for uncontrolled, LQ, and ES controlled wing.

Table 3 RMS loads at modified gust test condition ($M=0.7$, $h=4572$ m, $V_G=2.5$ m/s)

	root 1	2	Station 3	4	5	6	7	8	tip 9
Final LQ									
Bending moment, N-m	1729	1365	1032	736	413	268	114	25	2
Shear, N	561	502	442	381	261	220	140	40	20
Torque, N-M	11	16	22	25	22	19	16	2	1
Final ES									
Bending moment, N-M	1674	1329	1012	728	414	271	117	27	2
Shear, N	522	522	421	361	261	221	140	40	20
Torque, N-M	14	19	24	26	23	20	16	2	1
Open loop									
Bending moment, N-M	1670	1284	939	640	336	202	75	14	1
Shear, N	602	522	462	361	221	181	100	20	20
Torque, N-M	32	39	46	47	42	36	36	7	1

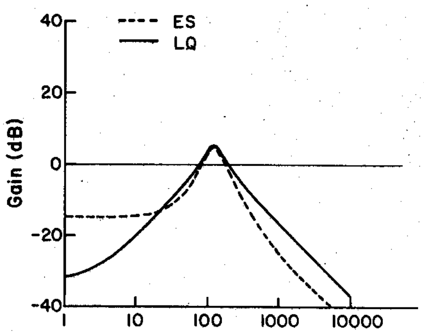

Fig. 7 Frequency response of magnitude of $H(s)\ G(s)$ for LQ and ES designs.

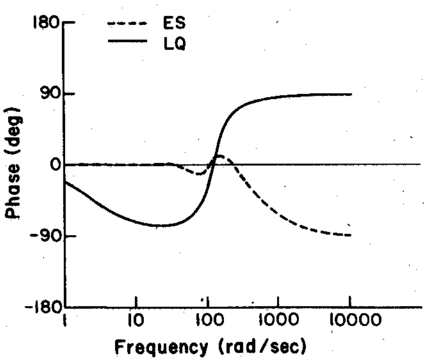

Fig. 8 Frequency response of phase of $H(s)G(s)$ for LQ and ES designs.

It is interesting to note that the actuator poles, the poles associated with the unsteady aerodynamic lag states, and all of the poles associated with the stable flexure modes have been canceled by zeros. The only remaining poles are those associated with the unstable first bending mode. Bode diagrams for the LQ loop transfer function are given in Figs. 7 and 8. The gain margin is 6 dB and the phase margins are greater than 60 deg. This is not surprising, since Safanov and Athans[21] show that full-state LQ controllers yield excellent gain and phase margins.

The loop transfer function for the ES controller is

$$H(s)G(s)_{\mathrm{ES}}=\frac{51.45(s-427.4)(s-66.5)(s+42.4)}{[s^2-79.8s+(124.5)^2]\,[s^2+188.6s+142.2)^2]}$$

Again, all of the actuator poles and the poles associated with the unsteady aerodynamic lag states have been canceled by zeros. But only the poles associated with the first torsion mode have been canceled and the unstable first bending mode and stable second bending mode remain. Bode diagrams for this transfer function are also shown in Figs. 7 and 8. The gain margins are 6 dB or better, but the phase margins are slightly less than 20 deg. Gain vs frequency plots for the LQ and ES transfer functions are very similar for frequencies above 10 rad/s. Both curves peak at the flutter frequency with a gain of 6 dB and then roll off rapidly with increasing frequency.

Conclusions

The eigenspace (ES) and linear quadratic (LQ) controllers give very similar results in terms of required control surface activity. At the gust test condition, the ES design exhibits lower wing root bending moment and shear than the LQ design, but the LQ controller provides slightly lower torsional stress. Both the ES and LQ designs provide significantly reduced torsional stress at the wing root, slightly reduced shear, and slightly increased bending moment compared with the open-loop response. Both the LQ and ES controllers significantly increased flutter speed compared with the uncontrolled wing. The ES controller results in a slightly greater flutter speed than the LQ controller. For a fixed Mach number, the ES design is stable at lower altitudes than the LQ design. The LQ design exhibits significantly better phase margins than the ES design at the flutter test condition. The gain margins are the same.

The LQ design requires large feedback gains on the inboard actuator states. This reduces the overall inboard actuator gain. Increased forward loop gain would be required to restore open-loop characteristics. This might necessitate redesign of existing actuator hardware. The ES controller does not require actuator feedback, and the closed-loop frequency response characteristics of the actuators is the same as the open-loop case. However, the phase margins are not adequate. The ES design technique developed does allow the achievement of desired rms response characteristics by eigenvector shaping and has promise for use in applications to other aeroelastic control problems.

An important conclusion is that the inboard control surface should not be used for flutter control. If the inboard aileron is included in the design, either the dynamic characteristics of the inboard actuator must be modified by feedback of actuator states (LQ design) or the stability margins must be sacrificed (ES design). As shown in Table 2, better performance is achieved if the inboard actuator is neglected. In this case, the LQ design results in all of the stable eigenvalues remaining in their open-loop configuration and the unstable eigenvalues being rotated about the imaginary axis. This controller will exhibit the same good gain and phase margins at the design condition, as shown in Figs. 7 and 8, and will also stabilize the wing at the gust test condition. Since the control is a scalar, the ES controller that rotates unstable roots about the imaginary axis and maintains the stable roots in their open-loop configuration is identical to the LQ controller. Currently, dynamic compensators that convert accelerometer output to outboard actuator input are being developed based upon full-state feedback control laws that accomplish the eigenvalue placement described above.

Acknowledgment

The results on ES design were obtained under Grant NAG-1-217 from NASA Langley Research Center. Mr. William Adams of NASA Langley and Mr. Sanjay Garg of the University of Minnesota were instrumental in developing and interpreting the mathematical models of the ARW-2. Mr. X.G. Li of the University of Minnesota played an important role in calculating the results for the LQ control system. Thanks are also due Dr. Thomas B. Cunningham of Honeywell Inc. for a number of useful discussions concerning eigenspace techniques.

References

[1]Murrow, H.N. and Eckstrom, C.V., "Drones for Aerodynamic and Structural Testing (DAST)—A Status Report," *Journal of Aircraft,* Vol. 16, Aug. 1979, pp. 521-526.

[2]Newsom, J.R., "Control Law Synthesis for Active Flutter Suppression Using Optimal Control Theory," *Journal of Guidance and Control,* Vol. 2, Sept.-Oct. 1979, pp. 338-394.

[3]Abel, I., Newsom, J.R., and Dunn, H.J., "Application of Two Synthesis Methods for Active Flutter Suppression of an Aeroelastic Wind Tunnel Model," AIAA Paper 79-1633, Aug. 1979.

[4]Mahesh, J.K., Stone, C.R., Garrard, W.L., and Dunn, H.J., "Control Law Synthesis for Flutter Suppression Using Linear Quadratic Gaussian Control Theory," *Journal of Guidance and Control,* Vol. 4, 1981, pp. 415-422.

[5]Mukhopadhyay, V., Newsom, J.R., and Abel, I., "Reduced-Order Optimal Feedback Control Law Synthesis for Flutter Suppression," *Journal of Guidance and Control,* Vol. 4, July-Aug. 1981, pp. 382-395.

[6]Gangsaas, D., Ly, U., and Norman, D.C., "Practical Gust Load Alleviation and Flutter Suppression Control Law Based on LQG Methodology," AIAA Paper 81-0021, Jan. 1981.

[7]Gangsaas, D. and Ly, U., "Application of a Modified Linear Quadradic Gaussian Design to Active Control of a Transport Airplane," AIAA Paper 79-1746, Aug. 1979.

[8]Moore, B.C., "On the Flexibility Offered by Full-State Feedback in Multivariable Systems Beyond Closed Loop Eigenvalue Assignment," *IEEE Transactions on Automatic Control,* Vol. 21, Oct. 1976, pp. 682-691.

[9]Ostroff, A.J. and Pines, S., "Application of Modal Control to Wing-Flutter Suppression," NASA Tech Paper 1983, May 1982.

[10]Garrard, W.L., Mahesh, J.K., Stone, C.R., and Dunn, H.J., "Robust Kalman Filter Design for Active Flutter Suppression Systems," *Journal of Guidance, Control, and Dynamics,* Vol. 5, July-Aug. 1982, pp. 412-414.

[11]Dowell, E.H., "A Simple Method for Converting Frequency Domain Aerodynamics to the Time Domain," NASA TM 81844, Oct. 1980.

[12]Garrard, W.L. and Liebst, B.S., "Eigenspace Techniques for Active Flutter Suppression," Dept. of Aerospace Engineering and Mechanics, University of Minnestoa, Minneapolis, Final Report, NASA Research Grant NAG-1-217, May 1982.

[13]Noble, B. and Daniel, J.W., *Applied Linear Algebra,* 2nd Ed., Prentice Hall, Englewood Cliffs, N.J., 1977, Secs. 9.6, 11.6.

[14]Adams, W.M. Jr. and Tiffany, S.H., "An Updated Comparison of NASA/Boeing Predictions of the Open Loop, Symmetric Flutter Characteristics of the DAST ARW-2," NASA Langley Research Center, Hampton, Va., APCO TM 81-1, Jan. 1981.

[15]Houbolt, J.C., Steiner, R., and Pratt, K.G., "Dynamic Response of Aircraft Due to Atmospheric Turbulence Including Flight Data on Input and Response," NASA TRR-199, June 1964.

[16]Li, X.G., "Combined Application of Optimal Regulator Theory and Frequency Domain Techniques to Design of a Flutter Control System," MS Thesis in Aerospace Engineering, University of Minnesota, Minneapolis, Sept. 1982.

[17]Kwakernaak, H. and Sivan, R., *Linear Optimal Control Systems,* John Wiley and Sons, New York, 1972.

[18]Cunningham, T.B., "Eigenspace Selection Procedures for Closed Loop Response Shaping with Modal Control," *Proceedings, IEEE Conference on Decision and Control,* Dec. 1980.

[19]Harvey, C.A. and Stein, G., "Quadratic Weights for Asymptotic Regulator Properties," *IEEE Transactions on Automatic Control,* Vol. 23, June 1978, pp. 378-381.

[20]Stein, G., "Generalized Quadratic Weights for Asymptotic Regulator Properties," *IEEE Transactions on Automatic Control,* Vol. 24, Aug. 1979, pp. 559-566.

[21]Safanov, M.G. and Athans, M., "Gain and Phase Margins of Multi-Loop LQG Regulators," *IEEE Transactions on Automatic Control,* Vol. 22, April 1977, pp. 173-179.